NJC

ROYAL SOCIETY OF CHEMISTRY

PAPER

Cite this: *New J. Chem.*, 2024, **48**, 2569

New nonlinear optical oxyfluoride $K_2NbO_2F_3$ with strong pseudo-centrosymmetry, obtained by mild hydrothermal synthesis†

Elena L. Belokoneva, *[a] Sergey Yu. Stefanovich,[b] Anatoly S. Volkov,[c] Olga V. Dimitrova[a] and Alexandra Mozgova[a]

Received 24th October 2023,
Accepted 3rd January 2024

DOI: 10.1039/d3nj04922a

rsc.li/njc

New polar $K_2NbO_2F_3$ crystals were obtained under mild hydrothermal conditions, which differ from the higher temperature synthesis of previously known Nb-containing oxyfluorides. X-ray diffraction analysis of the single crystal, performed in the polar space group $Pna2_1$, is consistent with the existence of the second harmonic generation (SHG) effect in powders. A monotonous increase in SHG power in samples with increasing powder grain size indicates phase matching of neodymium laser radiation and its second harmonic. However, SHG is relatively small and does not exceed a third of the intensity of standard KH_2PO_4 powders. The weakness of the second-order optical nonlinearity in K_2NbO_2F is related to the strong pseudo-symmetry of the crystal structure, corresponding to the space group $Pnam$-D_{2h}^{16}, and thus the structure is very close to centrosymmetric. Structural evidence for the polarity of the $K_2NbO_2F_3$ crystal is the subtle differences in the Nb–O bonds along the *c* axis in the (NbO_3F_3) octahedra, together with the presence of similar differences in the K1–O bonds. Extremely weak, close to the detection limit, very small deviations from the centrosymmetry of the entire structure also correlate with the existence of an almost second-order irreversible transformation of $K_2NbO_2F_3$ into a centrosymmetric phase at temperatures 50–60 °C below the decomposition temperature of the substance at 560 °C.

Introduction

Niobium is a rare element in the earth's crust, but many minerals containing it are widely known. They belong to various inorganic classes, mainly oxides, but also to silicates. There is lueshite $NaNbO_3$, loparite $(Na,Ce,Ca)(Ti,Nb)O_3$, columbite $(Fe,Mn)(Nb,Ta)_2O_6$, pyrochlore $(Ca,Na)_2Nb_2(O,OH,F)_7$, euxenite $Y(Nb,Ta)_2(O,OH,F)_6$, aeschynite $(Ca,Ca)(Nb,Ti)_2(O,OH)_6$, rare changbaiite $PbNb_2O_6$, frankonite $Na_2Nb_4O_{11}{\cdot}9H_2O$ and fergusonite $YNbO_4$.[1] Nb-silicates are also found: epistolite $Na_5TiNb_2[Si_2O_7](F/O_3){\cdot}5H_2O$, vuonnemite $Na_5TiNb_2[Si_2O_7](F/O_3){\cdot}2Na_3PO_4$, komarovite $(Ca,Mn)_2Nb_4[Si_4O_{12}]\ (F,O)_2O_6{\cdot}7H_2O$ or niobophyllite $(K,Na)_3(Fe,Mn)_7Nb_2[Si_4O_{12}]_2(OH,O)_7$, which contain Nb as one of the basic elements.[1] Columbite and aeschinite are of industrial importance. Isomorphic substitutions are characteristic of this element and are known for many minerals.

Nb-containing compounds have been synthesized not only as oxides and silicates, but also as germanates, borates, phosphates, fluorides, and iodates.[2] Most of them contain alkali metals – charge compensators, as in natural compounds. The complex electronic configuration of the Nb element results in polarization and the crystals often exhibit excellent nonlinear optical (NLO) properties. Some of the most attractive well-known materials are oxides $KNbO_3$[3] and $LiNbO_3$[4] with high optical nonlinearity, borate $CsNbO(B_2O_5)$[5] or silicate $K_2(NbO_2)$-Si_4O_{12}[6] and many others. Nb-octahedra (standard coordination of niobium) often have one short double bond, similar to Ti- or V-octahedra, and this configuration is characteristic of nonlinear crystals in the KTP structural family. The crystal $KTiOPO_4$ (KTP) with a titanyl bond was doped with Nb in an isomorphic ratio: $K_{0.84}(Nb_{0.08}Ti_{0.92})OPO_4$[7] to improve the properties. The crystals of this structure type are usually non-centrosymmetric. In particular, all members of the KTP family are ferroelectrics and regularly exhibit transformations between polar and centrosymmetric.[8] Due to their outstanding NLO characteristics, some of these crystals are widely used in photonic devices.

It is interesting to note the successful search for new silicates or germinates due to hetero-anionic motifs with the

[a] *Department of Crystallography and Crystal Chemistry, Geological Faculty, Lomonosov Moscow State University, Moscow, 119991, Russia. E-mail: elbel@geol.msu.ru; Tel: +7-495-939-4926*

[b] *Laboratory of Functional Materials, Chemical Faculty, Lomonosov Moscow State University, Moscow, 119991, Russia*

[c] *Skolkovo Institute of Science and Technology, Moscow, 121205, Russia*

† Electronic supplementary information (ESI) available: Additional tables. CCDC 2282508. For ESI and crystallographic data in CIF or other electronic format see DOI: https://doi.org/10.1039/d3nj04922a

introduction of S-atoms, which have high nonlinear optical properties and repeat mineral structure types or are completely new.[9–11]

Complex frameworks with two-dimensional channels are known for Nb-compounds with additional anionic groups, for example for silicate $Cs_3(NbO)_2[Si_8O_{21}]$[12] and germanate $K_3Nb_5GeO_{16}{\cdot}2H_2O$ which have ion-exchange properties.[13] Some compounds belong to the NASICON structure type or represent its ''empty'' structural variant as $Nb_2(PO_4)_3$;[14] $Na_3K_3Nb_8P_5O_{35}$[15] is niobium phosphate ''bronze''.

Unlike oxides, oxyfluorides are distinguished into a class of inorganic compounds combining O and F atoms as anions. They were found in nature and synthesized. Oxyfluorides have been known for a long time. We should mention A. F. Wells's book[16] in which this class of compounds was characterized. One of the first oxyfluorides with Nb was the ferroelectric Bi_2NbO_5F,[17] which was studied in detail later. However, many of the Nb-oxyfluorides have not yet been structurally studied, and their properties are not well known (see the review of some fluorides and oxyfluorides[18] and database[2]). Compounds and multicomponent compositions based on Nb-oxyfluorides are interesting mainly as glass-forming precursors for the creation of amorphous and glass-crystalline materials of near- and mid-IR photonics.[19–21] Compared to single crystals, oxyfluoride glasses are more technological and have a wider range of luminescence, laser generation and other useful properties associated with the possibility of introducing ions of rare-earth and transition metals or bismuth into their composition. In particular, the possibilities of creating light emitters and detectors based on oxyfluoride glass ceramics $M^{2+}NbOF_5$ (M^{2+} = Ba, *etc.*),[20] which have good glass-forming properties and allow the addition of bismuth trifluorides, indium, rare-earth elements, have been discussed in the literature.[22] The paucity of known oxyfluorides makes it difficult to optimize the preparation and properties of glass–ceramics based on them, since a high oxygen/fluorine ratio sharply deteriorates glass formation, and the reverse ratio adversely affects photoluminescence due to the usual centrosymmetry of their structures. The latter circumstance sharply weakens the luminescence of guest ions with D–D and D–F transitions especially in the case of these ions in the local center of symmetry where such transitions between electronic states are forbidden in the dipole approximation. Obtaining non-centrosymmetric oxyfluorides with optimized oxygen/fluorine ratio remains an important task in the creation of efficient glass-crystalline photonics materials.

Various methods for the synthesis of Nb-containing crystals have been used; one of the preferred ones is hydrothermal, which was carried out at high temperatures of 450–600 °C and pressures of 500–1500 atm. These parameters are due to the low solubility of Nb_2O_5 in aqueous solution. This oxide dissolves best in concentrated alkaline solutions as well as in hydrofluoric and oxalic acids.[23] Crystallization of Nb-compounds under mild middle-temperature conditions (T = 180 – 280 °C; P = 50 – 100 atm) is of great interest since it facilitates the preparation of new functional materials. Proper selection of mineralizers–components of the crystallization process, was one of the tasks of our research, the successful solution of which made it possible to improve the dissolution of Nb oxide in water at reduced temperature and pressure.

In this paper we detail of synthesis of $K_2NbO_2F_3$ under mild hydrothermal conditions, and describe its truly polar but very high pseudo-symmetrical crystal structure and nonlinear optical properties. Some correlations between structure and properties are also considered.

Experimental section

Single crystal growth

Single crystals of new oxofluoride $K_2NbO_2F_3$ were synthesized under mild hydrothermal conditions. To increase the solubility of Nb_2O_5 a highly concentrated KF solution was used. The initial composition consisted of a mixture of Nb_2O_5 : KF : I_2O_5 = 1 : 17 : 3 which in mass ratio corresponded to 0.5 g (1.88 mmol) Nb_2O_5, 2 g (34.42 mmol) KF and 1 g (6 mmol) I_2O_5. The initial mass was dissolved in distilled water, hermetically sealed in a high-pressure vessel made of stainless steel with a fluoroplastic coating with a capacity of 30 ml and kept at T = 260 °C and P = 100 atm for 18 days. Final cooling after synthesis to room temperature was carried out after 24 hours. The grown crystals were isolated by filtration of the initial solution, washed with hot water and dried in air.

Among the reaction products, two sorts of colourless transparent crystals immediately stand out. One of them was large and often formed splices elongated up to 3.51 mm with the cross-section up to 0.7 mm. The shape of individual rectangular crystals varies from bulk elongated prismatic block to thin-prismatic. That was type I phase. Initially less perceptible type II phase represented a small crystalline fraction by translucent and cloudy isometric crystals sometime similar to cubic. For both phases the mass yield of the experiment was close to ~90% at a ratio to each other of 1 : 1.

Phase diagnostics by powder diffraction and composition analysis

Phase diagnostics were carried out for both phases using selected morphological varieties of crystals of the types I and II. The second phase (type II crystals) is attributed to the known compound KIO_3 with high optical nonlinearity (30-940, JCPDF). They are pseudo-cubic, characterized in ref. 24 as really trigonal modification with space group $R3$. An experimental powder XRD pattern was obtained for morphologically separated crystals of type I phase using a STOE STADY diffractometer, with Cu-Kα (Fig. 1), which was new. The experimental picture agrees well with the simulated one calculated on the basis of crystal structure determination (see below) using the.cif file and the STOE XPow[25] program, Fig. 1. Thus, powder diffraction confirms the two-phase yield of hydrothermal synthesis, where, in addition to the well-known nonlinear optical iodate KIO_3, an equal amount of crystals, approximately, of a new individual phase were obtained. These crystals became the subject of our determination of the chemical formula and crystal structure.

Elemental analysis for the new phase was carried out on crystal surfaces on bulk prismatic and thin-prismatic individual

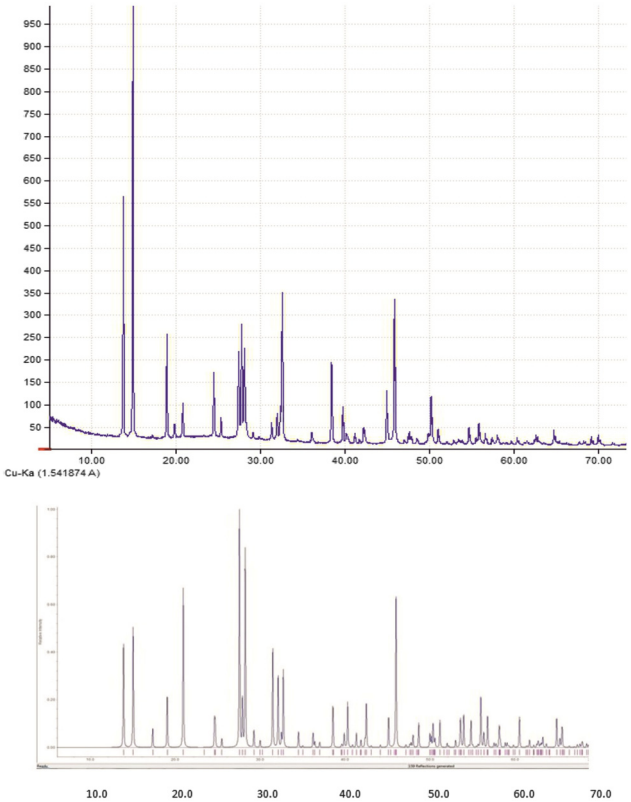

Fig. 1 Experimental powder diffraction pattern of $K_2NbO_2F_8$ crystals, STOE STADY diffractometer, Cu Kα-radiation, 2θ-interval 6–70.0° (top) and simulated (bottom) powder diffraction pattern, horizontal scale is 2θ-interval, vertical scale is reflection intensity.

crystals using a Jeol JSM-6480LV scanning electronic microscope in combination with WDX analysis. The test revealed the same composition with the presence of K, Nb, O and F. Determination of the structure (see below) showed it to be $K_2NbO_2F_3$. The oxyfluoride $K_2NbO_2F_3$ was previously chemically identified as a product of multiphase crystallization at T = 838 °C in the system KF-Nb_2O_5.[18] However, the X-ray pattern, unit cell parameters, and crystal structure were not determined.

Nonlinear optical properties

The second harmonic generation (SHG) study was applied to $K_2NbO_2F_3$ for controlling the non-centrosymmetry of the crystal structure and also for the classification of nonlinear optical properties. The nonlinear optical characteristics of the substances were firstly examined with the SHG powder technique by Kurtz and Perry[26] in the transmitted light geometry. However, in many cases Kurtz and Perry's method is more convenient in the reflection geometry,[27] since in this case the output SHG signal is independent of the thickness of the powder sample. The latter eliminates the need to use any immersion liquid and allows quantitative measurements of SHG in wide temperature intervals.

In our SHG experiments, laser impulses from a Minilite-I YAG:Nd-laser (Q-switched mode, repetition rate 10 Hz) were directed to $K_2NbO_2F_3$ powders previously separated according

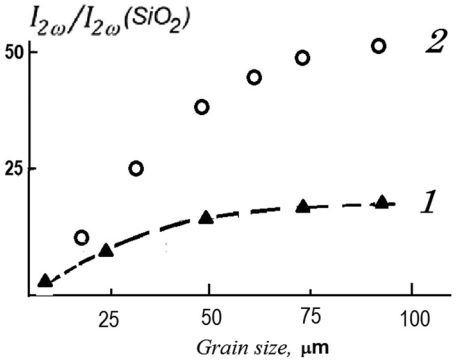

Fig. 2 SHG response of $K_2NbO_2F_3$ (1) in comparison with KH_2PO_4 (2) in dependence on average grain size in powders.

to grain size by sieves. Laser radiation with doubled frequency was registered by a photomultiplier tube in the backward direction to the laser beam. Thin powder of α-quartz with 3–5 μm grains was used as a standard sample in measuring SHG output $I_{2\omega}$ from all the powders. The results are shown in Fig. 2 for different grain-size powders of $K_2NbO_2F_3$ in comparison with similar dependences for typical NLO material KH_2PO_4 (KDP), which represents non-centrosymmetric crystals with so-called phase-matching (PM) properties. It follows from the data of Fig. 2 that the nonlinear optical activity of $K_2NbO_2F_3$ powders is smaller compared to KH_2PO_4, but shows a similar dependence on the grain size. The latter circumstance allows us to assert that the birefringence of these crystals is sufficiently large, since it is a necessary condition for the phase matching of YAG:Nd-laser radiation and its second harmonic.[26] The SHG-output of $K_2NbO_2F_3$ thin powder with a grain size of 5 μm is twofold higher than that of quartz, and this indicates a slightly higher value of its optical nonlinear coefficient d compared to quartz. According to our methodology,[24] the quantitative comparison of the d values is most valid for the finest powders in which the presence or absence of PM has a minimal effect on the value of $I_{2\omega}$. Using the tabulated value of d_{11} = 0.365 pm V^{-1} for α-quartz, an estimated value for space-averaged coefficient $\langle d \rangle$ = 0.5 pm V^{-1} can be obtained for the optical nonlinearity of $K_2NbO_2F_3$ which is just between α-SiO_2 and KH_2PO_4.

Phase thermal stability

Differential thermal analysis (DTA) was carried out in parallel with control of mass loss (MG) on STA 449 F3 Jupiter equipment (Netzsch, Germany) in the temperature range 30–1000 °C with a heating rate of 3 °C min^{-1} in an Ar atmosphere. Alumina crucibles were used. DTA/TG (curves 1, 2 in Fig. 3) indicates the beginning of the endopeak at 500 °C, which obviously corresponds to the decomposition of a substance with an extremum at 570 °C. In the range of 500–570 °C, the sample loses about 22% of its mass, which corresponds to defluorination. After this, the gradual evaporation of potassium oxide begins, followed by the formation of niobium oxide. Very close to the decomposition of $K_2NbO_2F_3$, the total mass loss reaches 56%. The decomposition of the sample continues in a wide temperature range from 500 to 1000 °C, which is the high-temperature limit of our thermal experiments.

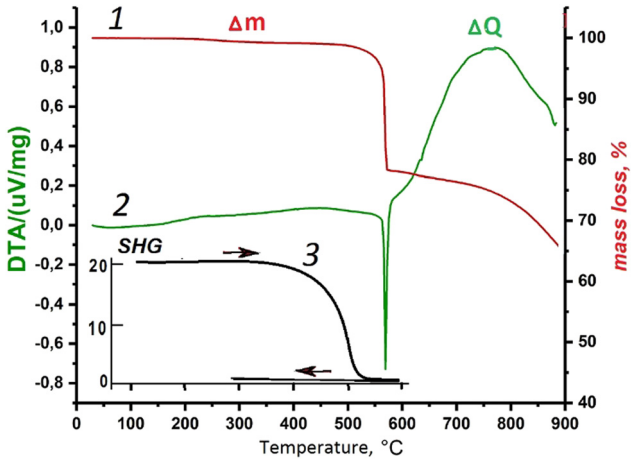

Fig. 3 DTA and DTG curves for $K_2NbO_2F_3$ on heating (1, 2 correspondingly) and SHG response from $K_2NbO_2F_3$ coarse powder on both heating and cooling (3) in units of SiO_2 standard powder signal.

Results and discussion

Single crystal X-ray diffraction and crystal structure analysis

The unit cell was determined for two colourless transparent crystals: bulk prismatic and fine prismatic using an XCalibur S diffractometer equipped with a CCD area detector (ω scanning mode) and graphite-monochromatic Mo Kα radiation source (λ = 0.71073 Å). The results were equal, revealing orthorhombic symmetry and no analogues compound was found in the ICSD database. The diffraction experiment was performed on the same diffractometer using a well faceted prismatic crystal shown in Fig. 4.

The data were integrated using the CrysAlisPro Agilent Technologies software[28] and corrected for the Lorentz and polarization factors. The crystal structure was solved using SHELXS[29] in polar space group $Pna2_1$ proposed by CrysAlis, which is consistent with the SHG signal. Three positions for heavy atoms were found: Nb, K1 and K2. Of the five anionic positions two were O1 and O2 atoms and three F1, F2 and F3 atoms: oxygens participated in the bridging bond Nb–O1–Nb and the double short bond Nb–O2. The model was neutral, based on Pauling's valence balance which allowed O- and F-atoms to be separated in the positions. However, for the confirmation of the assignment, bond valence sum parameters for all the atoms were calculated based on the empirical coefficients of Brese, and O'Keefe with both Nb–O and Nb–F bonds.[30] The values obtained correlate well with the expected valence state of all the atoms with the significant difference between O and F: Nb +4.5, K1 +1.0, K2 +1.055, O1 −2.085, O2 −1.78 (effect of double bond Nb–O2 is presented), F1 −1.25, F2 −1.18, F3 −0.98. The resulting chemical formula determined in structure refinement showed that it is a new oxyfluoride $K_2NbO_2F_3$, Z = 4. There were no reflexes in the reciprocal lattice that violated the found cell, and it was not possible to propose another variant of the structure. The refinement was performed using SHELXL[29] in an anisotropic approximation of temperature displacement parameters for all the atoms. Analysis of the structure drawn in WINATOM[31] clearly showed pseudo-mirror plane m_z on which the heavy atoms and two anions: O2 and F1 were almost located. Pseudo-symmetry with *Pnam* (*Pnma*-D_{2h}[16]) super-group was visible in the figure using initial atomic coordinates for all the atoms; however, with increasing refinement cycles, the *R*-factor decreased slightly and the positions of atoms became closer to centrosymmetric. This is explained by the known influence of pseudosymmetry in the least squares procedure. Checking for missing symmetry elements with the PLATON[32] program expectedly involved testing the centrosymmetric super-group *Pnam*. A control refinement in the supergroup with the new atomic positions gave equal *R*-factor, but this did not correspond to the properties of the crystals. Thus, the polar group $Pna2_1$ turned out to be correct with a rather rare case of very high pseudo-symmetry. Absorption correction was not performed because $\mu r_{av} < 1$ was insignificant, and it was also complicated to carry out facing of the crystal due to high shape anisotropy (crystal elongation corresponded to polar *c*-axis) which led to errors. No twinning was detected in the crystal in calculations. Accordingly to the Flack parameter 0.2(2), the absolute configuration was determined to be correct. Crystallographic data, atomic coordinates and selected bonds are presented in S1, S2, and S3 (ESI†); CCDC deposit number 2282508.†

The orthorhombic structure of the new oxyfluoride $K_2NbO_2F_3$ consists of Nb-octahedra joined at their vertices along the *c*-axis into zig-zag chains of 2_1-symmetry (Fig. 5a and b). $[NbO_2F_3]^{2-}$-chains are isolated from each other and located remotely in a checkerboard pattern in *ab*-projection (Fig. 5b). There is one short double bond Nb–O2 in the octahedron (shown by enlarged red ball) of 1.788 Å in length, which lies in a pseudo-mirror plane close to perpendicular to the polar *c*-axis. Two bridge bonds of magnitude Nb–O1 and O1′ of 1.90 (down polar *c*-axis) and 1.95 Å (up polar *c*-axis) (Fig. 5a) alternate along the polar *c*-axis. They are not equal to each other and when summed, create a resulting electric dipole responsible for the polarity of the whole crystal. If we estimate this difference before final refinements, it is larger and amounts to 0.1 Å. However, it is worth noting that this difference significantly exceeds the error of the X-ray experiment. The Nb–O bonds are slightly shortened compared to Nb–F bonds which have distances ranging from 2.00 to 2.12 Å (Table S3, ESI†), and nearly symmetrical along the *c*-axis. Large K cations at positions K1 and K2 unite these chains into a framework. Coordination numbers at distances up to 3 Å for K1 are CN = 6, and for K2 are CN = 7. The difference between bonds K1–O2 down the *c*-axis 2.87 Å and K1–O2′ up the *c*-axis 2.97 Å is

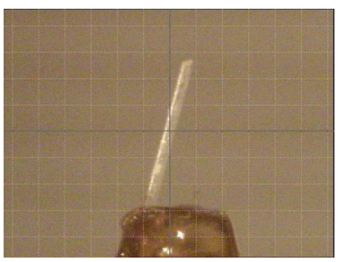

Fig. 4 Image of the crystal used in the diffraction experiment: a colourless transparent fine prismatic crystal with sizes of 0.05 × 0.08 × 0.6 mm.

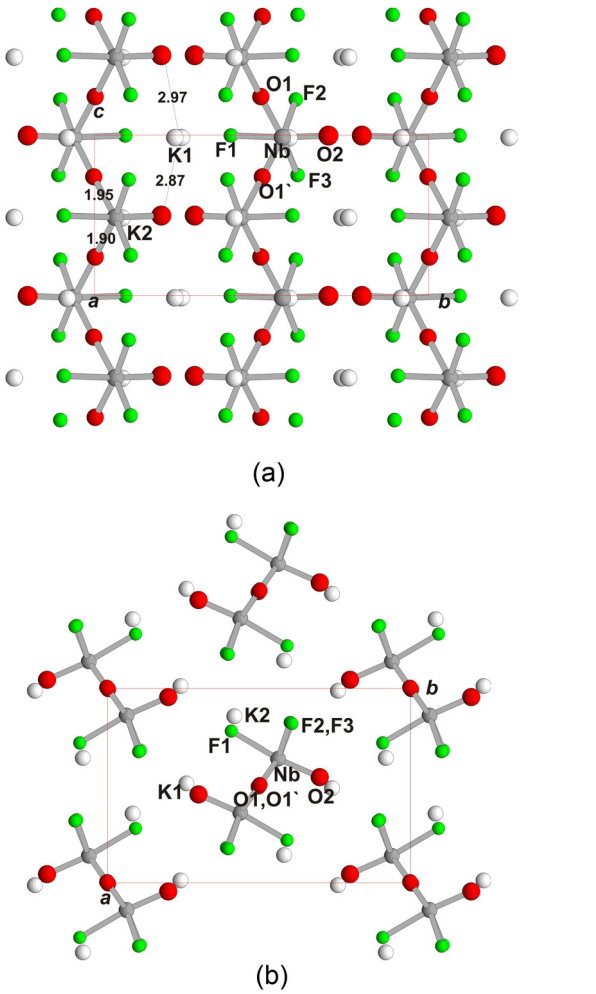

Fig. 5 Crystal structure $K_2NbO_2F_3$ in ball-and-stick presentation, K, Nb, F and O ions are shown by white, grey, green and red, respectively. Axes notations *a, b* and *c* are given. (a) Side view, characteristic bonds Nb–O1, Nb–O1′, K1–O2, and K1–O2′ different along the *c*-axis are shown, and (b) *ab*-projection.

again very noticeable (Fig. 5a). In addition, we note that the elongation and shortening of bonds are synchronized for Nb and K1 along the positive and negative *c*-axis directions. This structure makes it possible to determine the threshold at which polarity can be established under conditions of prevailing pseudosymmetry.

Structure–property relation

Conclusions about the presence of strong pseudosymmetry and its influence on the magnitude of the SHG signal were made earlier using examples of crystal structures of $BaOH(IO_3)$,[33] $Cs_3Ta(IO_3)_8$,[34] or Rb, Sc-iodates including $K_3In(IO_3)_6$.[35] Since the SHG properties of oxyfluorides have been poorly studied, let us compare the new oxyfluoride $K_2NbO_2F_3$ with the previously studied related ferroelectric $Rb_5Nb_3OF_{18}$.[36,37] In the polar space group *I*4*cm*, found for the latter, two independent Nb-atoms occupy special positions with different multiplicities: Nb1 at 8c on the *m* diagonal plane and Nb2 at 4a on the 4 fold axis at the beginning of the group. Thus, the number of Nb atoms for the tetragonal unit is 12. Nb1 is coordinated only by F atoms forming a distorted pentagonal bipyramid, CN = 7. Nb2 has four F and two O atoms, which form a tetragonal bipyramid or distorted octahedron with the oxygen vertices oriented along the *c*-axis. A short Nb2–O double bond with a length of 1.746 Å alternates with a long Nb–O′ bond with a length of 2.151 Å along the polar axis and explains the optical nonlinearity. Nevertheless, only a third (1/3) of the whole number of Nb atoms is responsible for the polar properties in $Rb_5Nb_3OF_{18}$.

In the new oxyfluoride $K_2NbO_2F_3$, all the Nb atoms possibly contribute to NLO properties. It is reasonable to assume that the double electron density of the Nb–O2 σ-bond has a π-component, which ensures charge (electron density) transfer along the Nb–O1–Nb–O1′ chain in the polar direction.

The new structure possesses a strong pseudosymmetry described by the *Pnam* supergroup (*Pnma*-D_{2h}[16]), which is predominantly determined in the X-ray experiment by the positions of heavy atoms. According to this, the noticeable SHG effect should be explained primarily by the deviation from pseudosymmetry in niobium octahedra. The deviation of pseudosymmetry in the Nb-octahedron is coupled in $K_2NbO_2F_3$ with a small but non-vanishing difference in the K1–O2 and K1–O2′ bonds down and up the *c*-axis. Increased bonds and shortened bonds are synchronized for Nb and K1 along the positive and negative *c*-axis direction, which ensures polarity.

Comparison in the Fig. 3 behavior of DTA and TG (curves 1 and 2) with dependence on temperature of the SHG signal (curve 3) shows the disappearance of SHG at approximately 500–510 °C, *i.e.* significantly lower than the destruction of the crystals at 560–570 °C. This disappearance of SHG indicates the presence of a specific phase transition in $K_2NbO_2F_3$, namely an irreversible phase transition from the RT-polar phase to the centrosymmetric phase at a temperature of about 500 °C. Probably, this transition can be initiated by a small loss of fluorine, as is clearly demonstrated by curve 1 at the same temperature. This means that even the slightest violation of the integrity of the $K_2NbO_2F_3$ crystal structure immediately leads to a loss of non-centrosymmetry.

Conclusions

Oxyfluorides as a class of compounds have been underexplored in recent years, and this new compound represents new crystals for both basic and applied research.

The successful crystallization of Nb compounds in mild medium-temperature conditions (T = 180–280 °C; P = 50–100 atm) indicates that the promising approach to the problem is associated with a choice of mineralizers. In this case, an excess of the KF component during the crystallization process provides better dissolution of the Nb_2O_5 oxide and crystallization of the compound.

The new crystal exhibits an extremely weak structural feature close to the detection limit – a small difference in the lengths of nonequivalent Nb–O bonds. In accordance with the small

difference in lengths, the weak SHG effect is limited by temperature and disappears 50–60 °C below the decomposition point of $K_2NbO_2F_3$. The disappearance of SHG is irreversible with temperature, exhibiting behavior different from conventional ferroelectric phase transitions.

The moderate optical nonlinearity discovered in $K_2NbO_2F_3$ is consistent with this structural feature. A small optical nonlinearity seems quite natural due to the very small deviation from the inversion center. More generally, any deviation from the inversion center of the entire structure as a whole can be considered as a result of differences in the lengths of certain bonds.

Author contributions

Conceptualization, EB, SS, AV and OD, methodology EB, SS, AV and OD, software EB, investigation EB, AV, SS, AM, resources EB, OD, AV, SS, writing-original draft preparation EB, AV, SS, writing review and editing EB, SS, AV, visualization EB, AM. All authors have read and agreed to the published version of the manuscript.

Conflicts of interest

There are no conflicts to declare.

Acknowledgements

The authors are grateful to Natalie Zubkova for her aid in collection of experimental diffraction and to the Laboratory of local methods of materials investigation, and to Vasilij Yapaskurt, geological faculty, MSU for the determination of compositions. This study was performed with the State assignment for Lomonosov Moscow State University in the theme "New minerals and synthetic analogues: crystallogenesis and crystal chemistry" (EB, SS, OD, AM).

References

1 H. Strunz and E. H. Nickel, Strunz Mineralogical Tables, *Chemical-Structural Mineral Classification System*, Schweizerbart, Stuttgart, 2001, p. 299.
2 Inorganic Crystal Structure Data Base – ICSD. Fachinformationzentrum (FIZ) Karlsruhe, 2011, I version.
3 A. W. Hewat, *J. Phys. C*, 1973, **6**, 2559–2572.
4 S. C. Abrahams, H. J. Levinstein and J. M. Reddy, *J. Phys. Chem. Solids*, 1966, **27**, 1019–1026.
5 P. Becker, L. Bohaty and R. Froehnlich, *Acta Crystallogr., Sect. C: Cryst. Struct. Commun.*, 1995, **51**, 1721–1723.
6 M. P. Crosnier, D. Guyomard, A. Verbare, Y. Piffard and M. Tournoux, *Ferroelectrics*, 1991, **124**, 61–66.
7 P. A. Thomas and B. E. Watts, *Sol. State Commun.*, 1990, **73**, 97–100.
8 E. L. Belokoneva, K. S. Knight, W. I. F. David and B. V. Mill, *J. Phys.: Condens. Matter*, 1997, **9**, 3833–3851.
9 Y.-F. Shi, Z. Ma, B. X. Li, X.-T. Wu, H. Lin and Q.-L. Zhu, *Mater. Chem. Front.*, 2022, **6**, 3054–3061.
10 M.-Y. Ran, S.-H. Zhou, B. Li, W. Wei, X.-T. Wu, H. Lin and Q.-L. Zhu, *Chem. Mater.*, 2022, **34**, 3853–3861.
11 M.-Y. Ran, S.-H. Zhou, W.-B. Wei, B.-X. Li, X.-T. Wu, H. Lin and Q.-L. Zhu, *Small*, 2023, **19**, 2300248.
12 M. P. Crosnier, D. Guyomard, A. Verbare and Y. Piffard, *Eur. J. Solid State Inorg. Chem.*, 1990, **27**, 435–442.
13 W. T. A. Harrison, T. E. Gier and G. D. Stucky, *J. Sol. State Chem.*, 1995, **115**, 373–378.
14 A. Leclaire, M. M. Borel, A. Grandin and B. Reveau, *Acta Crystallogr., Sect. C: Cryst. Struct. Commun.*, 1989, **45**, 699–701.
15 C. Gueho, M. M. Dorel, A. Grandin, A. Leclaire and B. Raveau, *Angew. Chem., Commun.*, 2019, **58**, 11666–11669.
16 A. F. Wells, *Structural Inorganic Chemistry*, Oxford University Press, Oxford England, 5th edn, 1986.
17 B. Aurivillius, *Arkiv four Kemi*, 1952, **4**, 39–47.
18 A. Agulyanski, *Crystal chemistry of tantalum and niobium fluoride compounds*, Elsevier BV, Amsterdam, 2004, pp. 257.
19 W. Ying, X. Fan, J. Gu, S. Xu and S. Liu, *Cell Rep. Phys. Sci.*, 2022, **3**, 100871.
20 P. P. Fedorov, A. A. Luginina and A. I. Popov, *J. Fluorine Chem.*, 2015, **172**, 22–50.
21 V. Nazabal, M. Poulain, M. Olivier, P. Pirasteha, P. Camy, J.-L. Doualan, S. Guy, T. Djouama, A. Boutarfaia and J. L. Adam, *J. Fluorine Chem.*, 2012, **134**, 18–23.
22 S. A. Polishthuk, L. N. Ignatieva, S. L. Sinebrjukhov, S. V. Gnedenkov, A. B. Podgorbunskij, N. N. Savchenko, A. B. Slobodjuk and V. M. Buznik, *Russ. J. Inorg. Chem.*, 2013, **58**, 387–391.
23 G. Deblonde, J.-P. Gauthier, D. Bengio, D. Beltrami, S. Bélair, G. Cote and A. Shagnes, *Sep. Purif. Technol.*, 2019, **226**, 209–217.
24 E. Belokoneva, S. Stefanovich and O. Dimitriva, *J. Sol. State Chem*, 2012, **195**, 79–85.
25 T. WinXPow, Stoe&CIE GmbH, Darmstadt, Germany, 2002.
26 S. K. Kurtz and T. T. Perry, A Powder Technique for the Evaluation of Nonlinear Optical Materials, *J. Appl. Phys.*, 1968, **39**, 3798–3813.
27 S. Y. Stefanovich, V. A. Morozov, D. A. Deyneko, E. A. Fortalnova, A. A. Belov, O. V. Barishnikova., A. A. Belik and B. I. Lazoryak, *J. Alloys Compd.*, 2018, **735**, 1826–1837.
28 *Agilent Technologies*, *CrysAlisPro Software System, version 1.171.3735*, Agilent Technologies UK Ltd., Oxford, UK, 2014.
29 G. M. Sheldrick, *SHELXL-97, a Program for Crystal Structure Refinement; SHELXS-97, a Program for Automatic Solution of Crystal Structures*, University of Goettingen, Goettingen, Germany, 1997.
30 N. E. Bresse and M. O'Keeffe, *Acta Crystallogr., Sect. B: Struct. Sci.*, 1991, **47**, 192–197, DOI: **10.1107/s0108768190011041**.
31 E. Dowty, *Atoms 3.2 – A Computer Program for Displaying Atomic Structures*, Kingpost, Kingpost, TN, USA, 1995.
32 A. L. Spek, *J. Appl. Crystallogr.*, 2003, **36**, 7–13.
33 O. Reutova, E. Belokoneva, A. Volkov and O. Dimitrova, *Symmetry*, 2021, **13**, 1477, DOI: **10.3390/sym13081477**.
34 E. L. Belokoneva, O. V. Reutova, O. V. Dimitrova, A. S. Volkov, S. Y. Stefanovich, V. V. Maltsev and M. F. Vigasina, *Cryst. Eng. Commun.*, 2023, **25**, 4364–4369, DOI: **10.1039/D3CE00461A**.

35 O. Reutova, E. Belokoneva, A. Volkov, O. Dimitrova and S. Stefanovich, *Symmetry*, 2023, **15**(1), 100, DOI: **10.3390/sym15010100**.
36 A. I. Agulyanskii, V. E. Zavodnik, U. V. Kuznetsov, N. V. Sidorov, S. Y. Stefanovich, D. A. Tsikaeva and V. T. Kalinnikova, *Izv. AN SSSR, Neorganich. Mater.*, 1991, **27**, 1055–1060.
37 A. I. Agulyanskii, Y. Stefanovich, D. A. Tsikaeva and V. T. Kalinnikov, *Izv. AN SSSR, Neorganich. Mater.*, 1991, **27**, 380–383.